

Fabrication and characterisation of hollow fibre ceramic membranes from fly ash

Siti Nur Afiqah Zulkifli, Azeman Mustafa*, Mohd Hafiz Dzarfan Othman*, Siti Khadijah Hubadillah

Advanced Membrane Technology Research Centre (AMTEC), Faculty of Chemical and Energy Engineering, Universiti Teknologi Malaysia, 81310 Johor, Johor Bharu.

* Corresponding author: r-azeman@utm.my, hafiz@petroleum.utm.my

Article history

Received 11 Mac 2019
 Revised 15 June 2019
 Accepted 1 January 2020
 Ublishe Online 17 August 2020

Abstract

The development of ceramic membrane to treat wastewater is generally limited due to the fact that materials commonly used for fabrication of these membranes such as high purity alumina (e.g. Al_2O_3) are expensive. Thus, the aim and purpose of this present work is to fabricate and characterize low-cost ceramic membranes using abundant and low-cost fly ash as the raw material. However, the presence of unburnt carbon in fly ash would significantly increase membrane porosity which would affect the mechanical strength and removal efficiency. Thus, it is of paramount importance to determine the optimum loading of fly ash during preparation of precursor solution. In the present work, the membrane precursors were prepared using three different fly ash loadings, i.e. 40wt%, 45wt%, and 50wt%. The membranes were fabricated via phase inversion technique and sintered at 1250°C. The membranes were then characterised in terms of its density, shrinkage, volumetric porosity, mechanical strength, and equilibrium water content. The results obtained show that at 45wt % loading, the membrane produced exhibited optimum properties with percent shrinkage, density, and bending strength of 52%, 1.28g/cm³, 37MPa, respectively. The higher shrinkage of 45wt% loading membrane as compared to other loadings also affects the cross-sectional morphology of membrane, exhibiting a spongy structure with smaller macrovoids at an average pore size of 7.8µm. In addition, the 45wt% loading membrane was also less porous as compared to other membranes, with 26% porosity and 39% to achieve equilibrium water content.

Keywords: Characterization, Fly Ash, Different loading.

© 2020 Penerbit UTM Press. All rights reserved

INTRODUCTION

Utilisation of fly ash has garnered interested in the industry, especially for research and development of ceramic products as fly ash has higher silica content. Higher content of silica in fly ash provides added value into the ceramic industry. Additionally, this allows fly ash to be a perfect replacement to alumina as the base material for development of ceramic membranes. Reviews done regarding fly ash have discussed on utilising fly ash in ceramic industrial Ahmaruzzaman, (2010); Wang & Wu, (2006); Yao et al., (2015) and also extracting desired metal from fly ash Blissett & Rowson, (2012); Mengfan et al., (2017). Cao et al. has successfully fabricated flat sheet ceramic membrane using fly ash by uniaxially pressing technique (Cao et al., 2014; Singh & Bulasara, 2013) and tubular membrane (Fang et al., 2011), but no research has been done for fabrication of ceramic hollow fibre membrane using fly ash. Besides, studies have successfully proven that fly ash can treat oily wastewater efficiently with 99% rejection (Fang et al., (2013; Suresh, Pugazhenthii & Uppaluri, (2016). Thus, the purpose of this study is to fabricate hollow fibre ceramic membrane based on fly ash via phase inversion technique.

However, some studies also reported that fabrication of fly ash ceramic membrane was not feasible since higher sintering temperature is required to increase its mechanical strength. Study done by Singh & Bulasara (2013) where they successfully fabricated fly ash membrane,

indicated that up to 65% of fly ash in membrane content comprised of calcium carbonate and sodium carbonate, boric acid to form metallic metaborates which led to improvement in mechanical strength of membrane. Sodium metasilicate acts as a binder by creating silicate bonds that induces higher mechanical strength. The results obtained indicated that with increasing temperature, the pore size of membrane becomes larger. At 800°C, 850°C, 900°C, and 1000°C, the pore size pattern is not of linear pattern as 1.524µm, 1.458µm, 1.202µm, and 2.301µm, respectively. This also directly affects the mechanical strength which was recorded at 8MPa to 20MPa. A study done by Dong et al. (2006) used dip-coating method to prepare a cordierite-based porous membrane by using fly ash as the ceramic material and magnesium carbonate as a source of magnesia to form the cordierite phase. Based on the linear shrinkage ratio curves for fly ash and magnesium, it was found that the samples with basic magnesium carbonate shrunk slightly in the range of 800–1080 °C and shrunk sharply between 1050 and 1200 °C, while the fly ash sample shrunk more than the others in the temperature range of 925–1370 °C. It is concluded that the samples with basic magnesium carbonate has a narrower sintering shrinkage range than pure fly ash samples. Thus, the mean pore size of the membranes increased in parallel to the increasing sintering temperature at 3.6µm, 4.1µm, 5.0µm, 6.4µm with increased sintering temperature of 1050°C, 1100°C, 1150°C, and 1200°C, respectively, due to presences of fly ash in the membrane.

In addition, based on the work by Cao et al. (2014) for the fabrication of membranes based on a mixture of fly ash and bauxite, they added 4% AlF_3 and 3% V_2O_5 as sintering aids which allow the membranes to be sintered at a higher temperature, in addition to contributing towards low pore size of $0.27\mu\text{m}$ at 1100°C and 59.5 MPa as compared to membrane sintered without the addition of AlF_3 and V_2O_5 ($0.57\mu\text{m}$ at 1100°C , 47.7MPa). However, the study also indicated that when sintered at higher temperature, such as 1400°C , the strength obtained was 78MPa but consist a large pore size at $0.94\mu\text{m}$. This may be due to the higher shrinkage contribute to the coalescences of particle necking at each other which leaves big pores behind. As for Shao, Jia & Liu, (2009), they used fly ash cenosphere FAC as a pore forming agent to fabricate porousness of Si_3N_4 ceramic by uniaxially pressed the mixed powder at 20MPa into pellets, then isostatically pressed at 150 MPa . They also investigated the effects of different fly ash content, either it was free of FAC at 5vol%, 10 vol%, 20vol%, or 30vol%. It was found that by increasing FAC content up to 30%, it caused a decrease in density, due to the hollow structure of FAC content, given that more spherical-shaped pores were formed on the pellet as increase in FAC content, median pore diameter concentrated at 630 nm , 530 nm , 600nm , and 800 nm .

Other than that, the presence on unburned carbon in fly ash from fluidised bed combustion, fly ash from pulverised fuel combustion, pressurised fluidised bed combustion, relationship of particle size of fly ash, and its loss of ignition contribute to the amount of unburned carbon in fly ash and bottom ash had been discussed by Bartoňová (2015). The presence of unburned carbon in fly ashes is problematic as this hinders further utilisation of these ashes in cement and construction material industry. They also review some technique to separate unburned carbon from fly ash and bottom ash by wet procedures (density separation, froth flotation, and oil agglomeration) or dry techniques (sieving, incipient fluidisation, and triboelectrostatic separations). They also emphasised on how the presence of unburned carbon in fly ash can be due to the design of combustion system and its operation. It was reported that unburned carbons could change the characteristics of a coal, especially its matter content and moisture content, of which affect other elements such as particle size. As discussed by Gao, Majeski and Runstedtler (2013), several factors that could come into play of unburned carbon's quantity in fly ash are residence time of coal in burning process, size of particles, and oxygen availability. As for its size, it is determined that small particles of coal contribute only 11% of carbon in ash from 65% carbon that present from coal entering the boiler. Additionally, it was also presented that the carbon content in ash will decrease when residence time increases as the particles do not have a longer time to react. Others major factor to the presence of carbon in ash was the oxygen availability, which in their case the carbon reduced from 3.27% to 1.3%. In another review, it was also stated that the unburned carbon have a strong influence to the adsorption capability such as adsorption of PCDD/F (Matzing et al., (2001), phosphate (Li et al., (2016; Li et al., (2006) and in other studies which reviewed the performance of adsorption capabilities by fly ash (Yao et al., (2015).

Next, Valderrama, Agredo & Gutiérrez (2011) studied the comparison between addition of fly ash (FA) and silica fume to concrete by investigating the effect on mechanical strength, capillary absorption, and chloride permeability. The result obtained showed that fly ash had low performance compare to silica fume and further addition of fly ash from 10% to 30% does not contribute to better performance. Thus, based on the previous studies to utilise fly ash to fabricate ceramic membrane, it is important to determine the content of fly ash to be used. This is because impurities such as hydrocarbons or unburned carbon in fly ash will affect the fabrication of fly ash ceramic membrane where there is the tendency to produce membrane of large pore size. Hence, it is important to determine the best loading of fly ash material for the fabrication of ceramic membrane, where the ideal amount of fly ash can contribute better pore size and mechanical strength without any addition of sintering aids such sodium metasilicate or boric acid or others additives for improved mechanical strength. The present study investigated the fabrication of fly ash in three different loading, which were 40wt%, 45wt% and 50wt% of fly ash via phase inversion techniques, at sintering temperature of 1250°C .

METHODOLOGY

Fabrication of Fly Ash Hollow Fibre Ceramic Membrane via Phase Inversion

The ash ceramic suspension was prepared with different loading of fly ash from 40wt%, 45wt% and 50wt% with the ceramic to polymer ratio maintained at 8:1. The dope compositions are presented in Table 1. In this study, fly ash as ceramic powder which was sampled from Kapar Energy Ventures Stesen Janaelektrik Sultan Salahuddin Abdul Aziz, Selangor Darul Ikhsan, was grinded and sieved to $<36\mu\text{m}$ particle size. The fly ash was kept dry in oven with temperature 60°C to avoid any moisture in the fly ash powder when applied for the fabrication. N-methylpyrrolidone (NMP, QR C^{TM}) as solvent, Polyethersulfone (PESf) (Radel A300, Ameco Performance, USA) as binding agent, and Arlcel P135 (Polyethyleneglycol 30 Dipolyhydroxystearate) as dispersing agent. According to the study of Kingsbury & Li, (2009), in the fabrication of ceramic membrane, polymer binder, PESf is capable of forming the best micro-channels structure during the conjunction between phase inversion and viscous fingering phenomenon. This polymer binder also acts to increase the viscosity and achieve a shear-thinning, so that the suspension is spinnable and fibre can be drawn through an orifice. The ceramic suspension for all three loadings was milled for 5 days in an alumina jar with four agate mill balls of 10mm size and one agate ball mill of 20mm size using a planetary ball mill (Model: NQM-2, Magna). The ceramic suspensions were used to fabricate hollow fibre membranes by dry wet spinning technique via phase inversion process. The critical point is spinning process, especially the rates of non-solvent (tap water) inflow during the extrusion spinning process or known as bore fluid rate. In this process, the tap water was used as internal flow during the suspension was extruded out as hollow fibre ceramic membrane. Thus, bore fluid rate for this study for tap water extrusion was 10ml/min with air gap distance between spinneret and coagulant bath were kept at 5 cm for all three loading that were fabricated. When the ceramic suspension was extruded out with water, there will be exchange between solvent in suspension and tap water inner of membrane. Thus, when solvent diffuses out from the suspension, and non-solvent (tap water) diffuses into the suspension, the finger-like formation or asymmetric structure will be created on the cross-sectional of the hollow fibre precursor (Paiman et al., (2015).

The produced membranes were then placed in an alumina crucible and sintered in a tubular furnace in the presence of air with 1250°C at intervals of 650°C for 2 h. The heating rate was set at 2°C min^{-1} from room temperature to 650°C and 3°C min^{-1} up to final temperature (1250°C)

Table 1 Composition of fly ash hollow fibre ceramic membrane at different loading.

Fly ash loadings	40wt%	45wt%	50wt%
Fly Ash powder (g)	40.00	45.00	50.00
PESf (g)	5.00	5.62	6.25
NMP(g)	54.00	48.38	42.75
Arlcel P135(g)	1.00	1.00	1.00

Density

Bulk density was calculated by measuring the dimension and weight which the bulk density, B, of a specimen in grams per cubic centimetre is the quotient of its dry weight (D) divided by the exterior volume (V), including pores. The density test was run for three times and formula of bulk density, B as follows:

$$B, \text{g/cm}^3 = D/V \quad \text{Eq (1)}$$

Shrinkage

The shrinkage of membrane was determined from the differences volume of membrane before and after being sintered at temperature 1250°C . All the three loading were tested for three times until small standard deviation was achieved.

Bending strength

The mechanical strength of the fabricated ceramic membranes was calculated by three-point bending Instron Model 5544 tensile test provided with a load cell for 1kN. A hollow fibre membrane sample of 4 cm length was placed on the sample holder. The bending strength, σ_F , was calculated from the following equation:

$$\sigma_F = \frac{8FLD}{\pi(D_o^4 - D_i^4)} \quad \text{Eq (2)}$$

where F is a measured force at which fracture take place (N), L is length of membrane (m), D_o is outer diameter (m) of membrane, and D_i is inner diameter (m) of membrane. The outer and inner diameters were measured by using a calliper.

Equilibrium Water Content (EWC)

It is important to perform the equilibrium water content (EWC) test in order to test the wettability of membrane which could affect the flux and antifouling ability of the membranes. Hollow fibre membranes were weighed in an electronic balance in wet state after removing any superficial water on membrane surface using a clean tissue paper. The wet membranes were dried in a vacuum oven for 24h at a temperature of 50–60°C and then weighed again in dry state. The EWC at room temperature was calculated as follows:

$$\frac{W_{wet} - W_{dry}}{W_{wet}} \times 100 \quad \text{Eq (3)}$$

where W_{wet} is weighed membrane at wet state and the W_{dry} is weighed membrane at dry state.

Volumetric Porosity

Porosity of the membrane plays an important role in permeation and separation performances. The membrane porosity was determined as follows:

$$\text{Porosity} = \frac{W_{wet} - W_{dry}}{\rho_w \times V} \quad \text{Eq (4)}$$

where, ρ_w is density (g/cm^3) of pure water at room temperature and V is volume of the membrane in wet state (cm^3). Formula for volume of Hollow Fibre membrane: $\frac{1}{4} (3.142) (OD^2 - ID^2) (\text{Length})$.

Mercury Porosimetry

The pore-size distribution was measured using mercury porosimetry (AutoPore IV 9500, Micromeritics, Norcross, Georgia, USA).

Water Flux

Water flux performance was measured through membrane under steady state condition and calculated by using:

$$L_p = Q/A.t.P$$

where L_p is the water permeability ($\text{L/h.m}^2.\text{bar}$), Q as the volume of water permeated through membrane (L), A as area of the membrane surface (m^2), t as the time taken (h), and P as the pressure (bar).

RESULTS AND DISCUSSION

Density and shrinkage

As depicted in Figure 1, the density and shrinkage of fly ash hollow fibre ceramic membrane in different loading are not parallel with the increase in fly ash loading onto ceramic membranes. However, the density was parallel with its shrinkage. The density of all three membranes increased as its shrinkage increased. The density of all three hollow fibre ceramic membrane was between 0.58g/cm^3 to 1.28g/cm^3 at sintering temperature 1250°C . According to a study done by Hubadillah et al. (2016), kaolin content increased as the membrane density increased. This phenomenon is similar with the present study as the increase in fly ash content between 40wt% to 45wt% in ceramic membranes increased the membrane density, which is also correlated with increase membrane shrinkage. The increase in membrane

shrinkage reduces the pore size and directly increases its density. As explained by Dong et al., (2006), during heat-treatment, membranes shrink rapidly. In the case for 45wt% and 50wt% fly ash ceramic membrane, the decrease in density and shrinkage was due to the formation of large pores, as seen in SEM image pictured in Figure 4. Based on the SEM images, 50wt% fly ash loading exhibited larger sized macrovoids as compared to 40wt% and 45wt% fly ash loading. The presence of large macrovoid decreased the density of membrane. This result is supported by the study done by Vasanth, Uppaluri & Pugazhenthii, (2011) that density of the clay membrane decreased due to formation of large pores. It also indicates that 50wt% of fly ash loading is not suitable for filtration, because the fly ash acts as a pore former to membrane rather than becoming a base for the ceramic membrane as seen in other studies by Cao et al., (2014) which added fly ash into bauxite membrane, and Shao, Jia & Liu, (2009) who fabricated porous silicon nitride membrane with addition of different amount of fly ash.

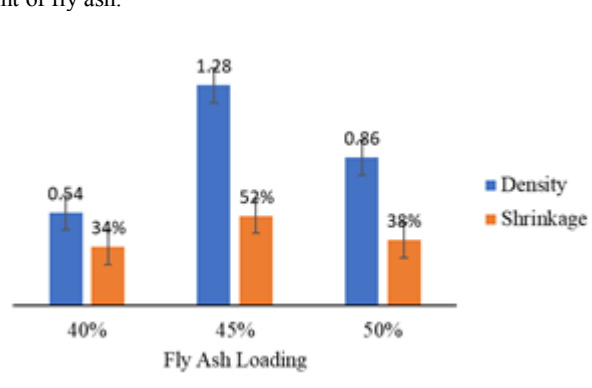


Figure 1 Relationship between density and shrinkage.

Bending strength and SEM image

Bending strength determination is important to determine the ability of membrane to perform at high pressure for gas or water permeation. Bending strength exhibited in Figure 3 indicates that 40wt% fly ash loading is not good enough for membrane filtration, since it has low bending strength as compared to other fly ash loadings, where bending strength of 25MPa for 40wt% fly ash loading, 37MPa for 45wt% fly ash loading and 33MPa for 50wt% fly ash loading were recorded.

Besides, the bending strength of 45wt% fly ash loading at 1250°C sintering temperature is better compared to results discussed by Dong et al., (2010) where fabrication of fly ash with 6% addition of titanium dioxide that acts as sintering aid achieved a mechanical bending strength of 36.05 MPa at sintering temperature of 1450°C .

Relating to the SEM image exhibited in Figure 4, the micrograph supports the bending strength result of 40wt% fly ash loading as it has large macrovoids as compared to 50wt% fly ash loading. This large macrovoids contributes towards the low bending strength exhibited by the membrane. Comparing both 45wt% and 50wt% fly ash loading, cross section of SEM images for both membranes are spongy in structure without the presence of small or big macrovoids. However, we can describe that, consolidation of microstructure in 50wt% fly ash loading does not completely occur, as it can be seen that 45wt% fly ash loading present more necking formation for adhesion of microstructure and formed dense membrane as compared to 50wt% fly ash loading which would require higher sintering temperature to shrink the microstructure and form a denser structure. It was also reported that Bonekamp (1996) there must be sufficient sintering or chemical bonding or interlocking of the membrane material during application. However, possible coalescence of microstructure should not lead to decreased permeability or defects in the membrane system such as micro-cracks.

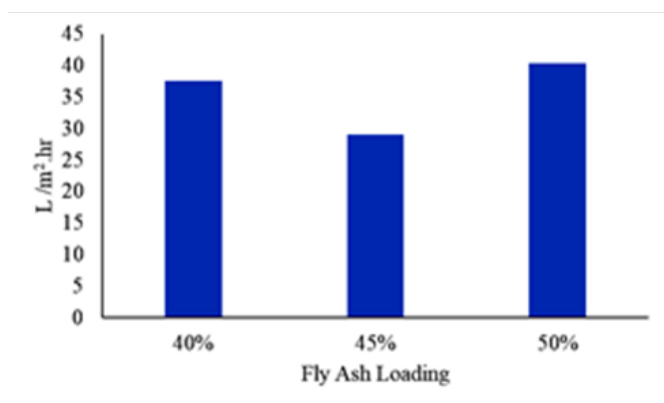


Figure 2 Water flux in different loading.

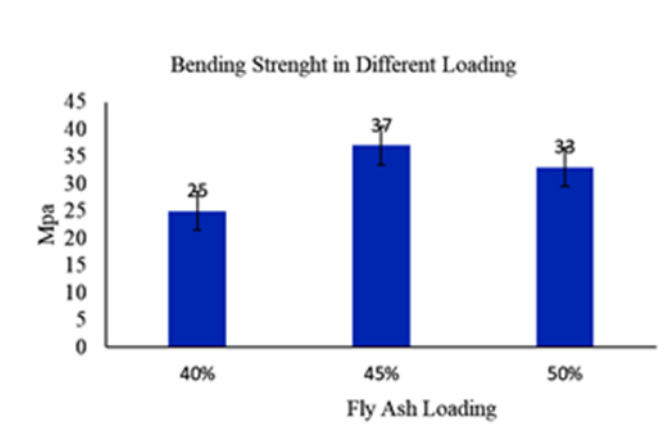


Figure 3 Bending strength in different loading.

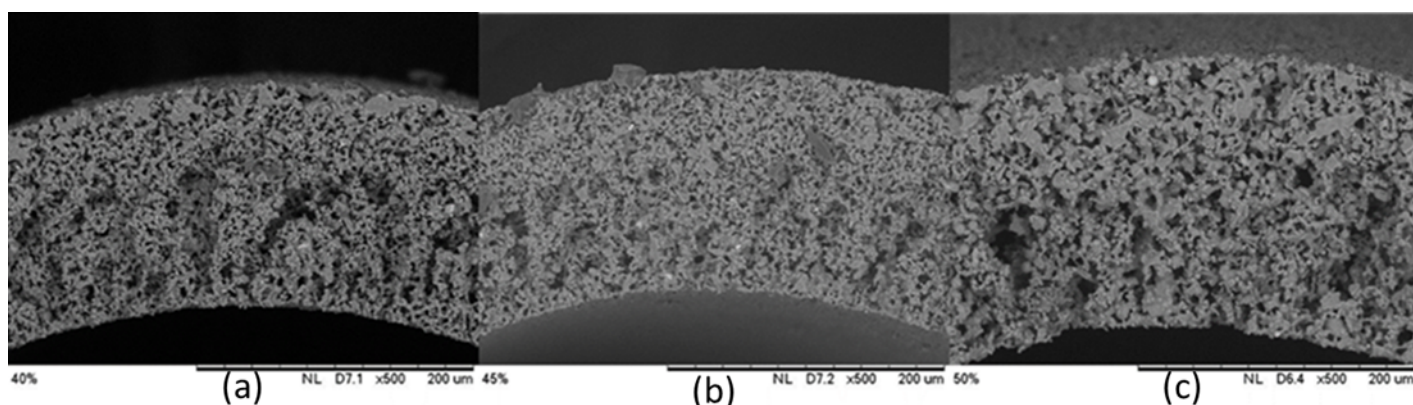


Figure 4: Cross-section image for all three loadings a) 40% fly ash loading, (b) 45% fly ash loading, (C) 50% fly ash loading

Based on the study conducted by Zulkifli et al. (2019), higher fly ash loading does not encourage phase inversion to occur due to the higher viscosity of ceramic suspension. This also is the main reason for the formation of spongy structure on the cross-section morphology of 45wt% and 50wt% fly ash loading ceramic membrane and the presence of some of large macrovoids on the cross-section morphology of 40wt% fly ash loading. In addition, Ricahrd (2012) stated that increase of dope viscosity will reduce precipitation rate and attributes to the increased shear and elongation viscosities. This would then in turn induce greater degree of chain entanglement, will reduces nonsolvent penetration to leach out during coagulation of ceramic suspension due to the resistance that disturbs the stability of suspension. Then, the hindrance for phase inversion changes from one phase solution to two phases, which are ceramic rich phase to form solid matrix of membrane and the other phase is the ceramic poor phase to form the membrane pores or macrovoids. Other than that, the ceramic phase also may contain some hydrocarbon such as unburned carbon from the fly ash itself, polymer binder (PESf), and other metal oxide that will be burned away when sintered at 1250°C and create a vacant space to the cross section of hollow fly ash ceramic membrane. The vacant space due to decomposition of polymer binder was also reported by Abdullah et al. (2016) where different ceramic to polymer ratio contributed to the formation of macrovoids. In this present study, increasing the fly ash loading also increases the polymer binder support, which is the reason why the cross-section images for 50wt% fly ash, exhibited larger vacant space as compared to 45wt% fly ash loading, and require higher temperature to completely burn any present carbon in 50wt% fly ash membrane. Figure 2 shown the result of water flux in different loading after 90 minutes of filtration. The 45wt% fly ash loading obtained lowest water flux as 29 L/ m².hr, followed by 40wt% and 50wt% with the amount 37.58 L/m².hr and 40.38 L/ m².hr, respectively. Parallel with result of SEM image and mercury porosimetry, the spongy structure with smaller pore size in 45wt% fly ash loading provide resistance for water permeation and decreased the water flux of membrane. The smaller pore size gives more space for holding water

molecule compare to higher pore size would tend to let the water out from the membrane matrix.

Volumetric porosity and equilibrium water content

Figure 5 shows that 45wt% fly ash loading had low volumetric porosity of 26%, followed by 40wt% and 50wt% fly ash hollow fibre ceramic membrane which exhibited values of 29% and 43% of porosity, respectively. The result of equilibrium water content was similar, where 50wt% fly ash loading exhibited higher water content as compared to 40wt% to 45wt% fly ash hollow fibre ceramic membrane, with values of 53%, 39% and 64% for 40wt%, 45wt% and 50wt% fly ash loading, respectively. According to the study done by Kumar et al.,(2017), decreasing equilibrium water content decreases the porosity of membrane. This indicates that the 50wt% fly ash membrane is more porous membrane, followed by 40wt% and 45wt%.

Results of equilibrium water content strongly support the porosity of membrane Ju et al., (2009) because the membrane is capable to withhold larger amount of water content due to presences of higher number of pores that can accommodate water molecules in the membranes. Additionally, other study reported that the equilibrium water content in membrane can be increased via the addition of pore former. The study done by Jasiewicz and Pietrzak, (2013) used polyvinylpyrrolidone (PVP) as a pore former to achieve 78% equilibrium water content, and another study done by Chakrabarty, Ghoshal & Purkait, (2008) reported that for PSf/NMP/PEG membranes, the EWC for PEG 400 is 56.8%, for PEG 6000 is 68.2% and for PEG 20000 is 78.8%. Similar trends were also seen for PSf/DMAc/PEG membranes, where for addition of PEG 400 it was 58.6%, for PEG 6000 it was 69.1% and for PEG 20000 it was 76.4%. We also can justify that 50wt% fly ash loading in fabrication of ceramic membrane not only acts as a ceramic material for the preparation of fly ash hollow fibre ceramic membrane, but also indirectly acts as a pore former.

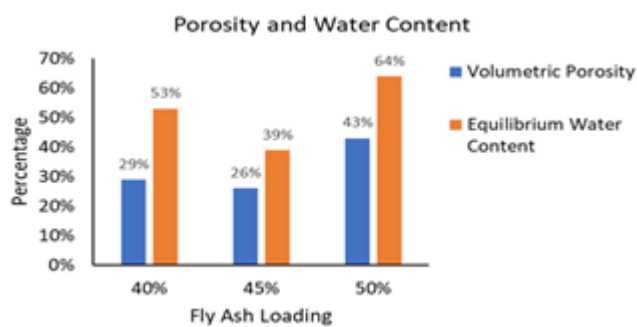


Figure 5 Comparison between volumetric porosity and equilibrium water content in three different loadings.

Next, mercury porosimetry analysis from Figure 6 shows that for all the three loadings of fly ash ceramic membranes consist of minimum pore size as $7.8\mu\text{m}$. This classifies all the three fly ash hollow fibre ceramic in the microfiltration range and as a mesoporous membrane due to the pore size more $>1\mu\text{m}$. Figure 6 also depicts that 50wt% fly ash membrane encountered higher volume of mercury intrusion at $7.4\mu\text{m}$ as compared to other membrane, which also indicates that the 50wt% fly ash consists of higher pore volume at pore size $7.8\mu\text{m}$ compare to other membrane. Nevertheless, the fly ash hollow fibre ceramic membrane cannot challenge other membrane which had pore size with nanofiltration or ultrafiltration range. This mesoporous of fly ash hollow fibre ceramic membrane potential to acts as hybrid method with adsorption and filtration process. From the previous study by Zulkifli et al. (2019), the presences of mullite ($2\text{Al}_2\text{O}_3 \cdot \text{SiO}_2$), antrigote ($3\text{MgO} \cdot \text{SiO}_2 \cdot 2\text{H}_2\text{O}$), and Pyrophyllite ($\text{Al}_2\text{O}_3 \cdot 4\text{SiO}_2 \cdot \text{H}_2\text{O}$) which change silanol and alumino to negative charge as SiO_2^- and AlO^- are capable to adsorbed the cationic charge. This adsorption study by silica and alumina successfully done by Gucek et al. (2005) and Kremleva et al. (2012).

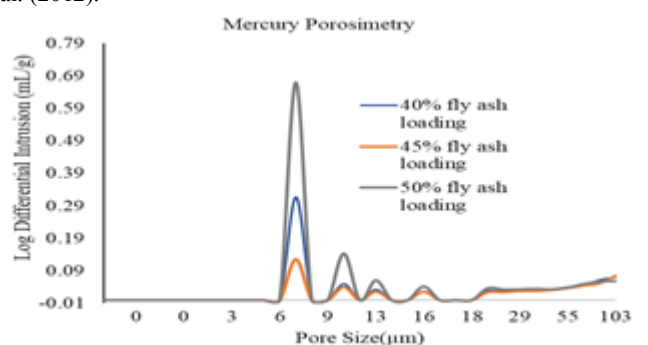


Figure 6 Pore size of fly ash hollow fibre ceramic membrane in different loading.

CONCLUSION

The optimum loading for the fabrication of fly ash hollow fibre ceramic membrane was 45wt%, with 52% of shrinkage, $1.28\text{g}/\text{cm}^3$ of density of and mechanical strength of 37 Mpa. It was also performed with low membrane porosity and equilibrium water content of 29% and 36% respectively. Lastly, further study for reducing the level of unburned carbon, such as flotation, should also be considered to improve fly ash quality.

ACKNOWLEDGEMENT

This work was financially supported by the Universiti Teknologi Malaysia under Higher Institution Centres of Excellent (HICoE) grant (Project Number: R.J090301.7846.4J205).

REFERENCES

- Abdullah, N., Rahman, M. A., Othman, M. H. D., Ismail, A. F., Jaafar, J., Aziz, A. A. (2016). Preparation and characterization of self-cleaning alumina hollow fiber membrane using the phase inversion and sintering technique. *Ceramics International*, 42(10), 12312-12322.
- Ahmaruzzaman, M. (2010). A review on the utilization of fly ash. *Progress in Energy and Combustion Science*, 36(3), 327-363.
- Bartoňová, L. (2015). Unburned carbon from coal combustion ash: An overview. *Fuel Processing Technology*, 134, 136-158.
- Blissett, R. S., Rowson, N. A. (2012). A review of the multi-component utilisation of coal fly ash. *Fuel*, 97, 1-23.
- Bonekamp, B. C. (1996). Preparation of asymmetric ceramic membrane supports by dip-coating. In A. J. Burggraaf & L. Cot (Eds.), *Fundamentals of Inorganic Membrane Science and Technology* (Vol. 1, pp. 141-225). Netherlands: Elsevier Science B. V.
- Cao, J., Dong, X., Li, L., Dong, Y., Hampshire, S. (2014). Recycling of waste fly ash for production of porous mullite ceramic membrane supports with increased porosity. *Journal of the European Ceramic Society*, 34(13), 3181-3194.
- Chakrabarty, B., Ghoshal, A. K., Purkait, M. K. (2008). Effect of molecular weight of PEG on membrane morphology and transport properties. *Journal of Membrane Science*, 309(1-2), 209-221.
- Dong, Y., Hampshire, S., Zhou, J. E., Lin, B., Ji, Z., Zhang, X., Meng, G. (2010). Recycling of fly ash for preparing porous mullite membrane supports with titania addition. *Journal of Hazardous Materials*, 180(1-3), 173-180.
- Dong, Y., Liu, X., Ma, Q., Meng, G. (2006). Preparation of cordierite-based porous ceramic micro-filtration membranes using waste fly ash as the main raw materials. *Journal of Membrane Science*, 285(1-2), 173-181.
- Fang, J., Qin, G., Wei, W., Zhao, X. (2011). Preparation and characterization of tubular supported ceramic microfiltration membranes from fly ash. *Separation and Purification Technology*, 80(3), 585-591.
- Fang, J., Qin, G., Wei, W., Zhao, X., Jiang, L. (2013). Elaboration of new ceramic membrane from spherical fly ash for microfiltration of rigid particle suspension and oil-in-water emulsion. *Desalination*, 311, 113-126.
- Gao, H., Majeski, A. J., Runstedler, A. (2013). A method to target and correct sources of unburned carbon in coal-fired utility boilers. *Fuel*, 108, 484-489.
- Gucek, A., Sener, S., Bilgen, S., Mazmanci, M. A. (2005). Adsorption and kinetic studies of cationic and anionic dyes on pyrophyllite from aqueous solutions. *J Colloid Interface Sci*, 286(1), 53-60.
- Hubadillah, S. K., Harun, Z., Othman, M. H. D., Ismail, A. F., Gani, P. (2016). Effect of kaolin particle size and loading on the characteristics of kaolin ceramic support prepared via phase inversion technique. *Journal of Asian Ceramic Societies*, 4(2), 164-177.
- Jasiewicz, K., Pietrzak, R. (2013). Metals ions removal by polymer membranes of different porosity. *Scientific World Journal*, 2013, 957202.
- Ju, H., McCloskey, B. D., Sagle, A. C., Kusuma, V. A., Freeman, B. D. (2009). Preparation and characterization of crosslinked poly(ethylene glycol) diacrylate hydrogels as fouling-resistant membrane coating materials. *Journal of Membrane Science*, 330(1-2), 180-188.
- Kingsbury, B. F. K., Li, K. (2009). A morphological study of ceramic hollow fibre membranes. *Journal of Membrane Science*, 328(1-2), 134-140.
- Kremleva, A., Martorell, B., Kruger, S., Rosch, N. (2012). Uranyl adsorption on solvated edge surfaces of pyrophyllite: a DFT model study. *Physical Chemistry Chemical Physics (PCCP)*, 14(16), 5815-5823.
- Kumar, S., Nandi, B. K., Guria, C., Mandal, A. (2017). Oil Removal from Produced Water by Ultrafiltration using Polysulfone Membrane. *Brazilian Journal of Chemical Engineering*, 34(2), 583-596.
- Li, F., Wu, W., Li, R., Fu, X. (2016). Adsorption of phosphate by acid-modified fly ash and palygorskite in aqueous solution: Experimental and modeling. *Applied Clay Science*, 132-133, 343-352.
- Li, Y., Liu, C., Luan, Z., Peng, X., Zhu, C., Chen, Z., . . . Jia, Z. (2006). Phosphate removal from aqueous solutions using raw and activated red mud and fly ash. *Journal of Hazardous Materials*, 137(1), 374-383.
- Matzing, H., Baumann, W., Becker, B., Jay, K., Paur, H. R., Seifert, H. (2001). Adsorption of PCDD/F on MWI fly ash. *Chemosphere*, 42(5-7), 803-809.
- Mengfan, G., Qingliang, M., Qingwen, L., Jiali, C., Hongzhu, M. (2017). A novel approach to extract SiO_2 from fly ash and its considerable adsorption properties. *Materials & Design*, 116, 666-675.
- Paiman, S. H., Rahman, M. A., Othman, M. H. D., Ismail, A. F., Jaafar, J., Aziz, A. A. (2015). Morphological study of yttria-stabilized zirconia hollow fibre membrane prepared using phase inversion/sintering technique. *Ceramics International*, 41(10), 12543-12553.
- Ricahrd, W. B. (2012). *Membrane Technology In Membrane Technology and Applications Membrane Technology* (Third Edition ed., Vol. 15). United Kingdom: John Wiley & Sons.
- Shao, Y., Jia, D., Liu, B. (2009). Characterization of porous silicon nitride ceramics by pressureless sintering using fly ash cenosphere as a pore-forming agent. *Journal of the European Ceramic Society*, 29(8), 1529-1534.

- Singh, G., Bularasa, V. K. (2013). Preparation of low-cost microfiltration membranes from fly ash. *Desalination and Water Treatment*, 1-9.
- Suresh, K., Pugazhenth, G., Uppaluri, R. (2016). Fly ash based ceramic microfiltration membranes for oil-water emulsion treatment: Parametric optimization using response surface methodology. *Journal of Water Process Engineering*, 13, 27-43.
- Valderrama, C. P., Agredo, J. T., Gutiérrez, R. M. d. (2011). A high unburned carbon fly ash concrete's performance characteristics. *Ingeniería E Investigación*, 31(1), 39-46.
- Vasanth, D., Uppaluri, R., Pugazhenth, G. (2011). Influence of sintering temperature on the properties of porous ceramic support prepared by uniaxial dry compaction method using low-cost raw materials for membrane applications. *Separation Science and Technology*, 46(8), 1241-1249.
- Wang, S., Wu, H. (2006). Environmental-benign utilisation of fly ash as low-cost adsorbents. *Journal of Hazardous Materials*, 136(3), 482-501.
- Yao, Z. T., Ji, X. S., Sarker, P. K., Tang, J. H., Ge, L. Q., Xia, M. S., Xi, Y. Q. (2015). A comprehensive review on the applications of coal fly ash. *Earth-Science Reviews*, 141, 105-121.
- Zulkifli, S. N. A., Azeman, M., Othman, M. H. D., Hubadillah, S. K. (2019). Characteristic properties of ceramic membrane derived from fly ash with different loadings and sintering temperature. *Malaysian Journal of Fundamental and Applied Sciences (MJFAS)*, 15(3).